COMPUTATIONAL INVESTIGATION OF VIBRATION CHARACTERISTICS ANALYSIS
FOR INDUSTRIAL ROTOR

Noureddine AIMEUR[*] , **Noureddine MENASRI**[*]

[*]Laboratory of Materials and Structural Mechanics, University of Mohamed BoudiafM'sila,
B.P 166 Ichbilia, M'sila, 28000, Algeria

noureddine.aimeur@univ-msila.dz; noureddine.menasri@univ-msila.dz

Abstract: During the operation of a rotor, various types of vibrations appear in this mechanical system and often limit the performance and endanger the safety of the operation. Therefore, dynamic analysis is essential because precise knowledge of the vibration behaviour is essential to ensure proper operation. This article presents a set of scientific techniques for the modelling and simulation of rotor vibrations. To work out the equations of the vibratory movement of the rotor, we used the energy approach of Lagrange. To achieve this, a model with one blading wheel carried by a shaft supported by two hydrodynamic bearings is chosen basedon the characteristics of the rotor studied (Fan 280 cement draft fan). It is an arduous task to manually ascertain the analytical resolution of the differential equations that characterise the vibratory behaviour of the rotor. The numerical approach employing the finite element method, programmed on the ANSYS software, made it possible to perform the vibration analysis of the rotor. First, the FAN 280 cement draft fan rotor is modelled using SolidWorks 3D software and reverse design using the coordinate measuring machine (CMM) for the design of the fins. Then, the modal characteristics of the fan rotor model were analysed using the finite element analysis (FEA) software ANSYS Workbench. Also, to study the effect of blade wear on critical speeds, the Campbell diagram was obtained. Finally, harmonic analysis was performed to determine the amplitude of the rotor vortex at critical speeds obtained with and without blade wear.

Key words: rotor dynamic, finite element method,reverse design (CMM), unbalanced,blade wear, simulation (ANSYS)

1. INTRODUCTION

Humanity is surrounded by rotating machines such as fans, pumps, compressors and gas turbines, whose successful operation depends on the behaviour of these machines and their components under dynamic conditions. Excessive vibration of rotating machines may in some cases not only harm the health of their operators but also result in a significant loss of productivity and/or product quality, and in consequence, a reduction in the reliability of machine components. Thus, to avoid these problems, it is essential to determine the excessive operating conditions for each machine operating under critical conditions [1-3].

The analysis of the dynamic characteristics of a machine mainly adopts the methods of experimental modal analysis and (FEM) modal analysis [4-10].

In recent years, there has been much research carried out in the field of the vibratory behaviour of rotors supported by bearings, resultant to which several theoretical and experimental developments and research findings have emerged.

Nan et al. [11] analysed the vibration characteristics of a horizontal machining centre.

By employing experimental modal tests, reliable modal parameters and dynamic characteristics can be obtained for the machining centre. Khan et al. [12], Khamari et al. [13] and Bai et al. [14] performed modal analysis to ascertain the natural frequencies and harmonic analysis using which to plot the stress and deflection at critical speeds. Accordingly, dynamic analysis of the rotor was performed in ANSYS APDL and Workbench to ascertain

the natural frequencies and critical speeds.

Several papers have dealt with the study of the dynamic behaviour of the unbalanced rotor [15-18]. The results show that the sudden unbalance in the operating system will cause larger oscillations, which are increased with the advance of the sudden unbalance; and the impact effect will be induced as a result, while the critical speed frequency is excited in the frequency spectrum.

Shuming and Yujia [19] have investigated the damping optimisation of high-pressure rotor support based on harmonic response analysis. The simulation results show that the parametric design of the supporting damping of the high-pressure rotor can effectively reduce the vibration of a high-pressure rotor passing the critical speed. Khamari et al. [13] and Nagaraj et al.[20] have presented the rotordynamic analysis of the rotor using the commercial finite element analysis (FEA) software ANSYS. Several authors in their contributions comprising the literature opine that the detailed (FEA) will be quite useful for researchers around the world. From the modal and harmonic analysis, it was seen that the turboexpander model is safe to operate at its designed rotational speed.Xu and Wang [21] propose an efficient method for free vibration analysis of rotating beams under elastic boundary conditions.

This paper presents a dynamic study of an industrial rotor (FAN280 cement draft fan). First, the FAN 280 cement draft fan rotor is modelled using SolidWorks 3D software and reverse design (CMM, for blade design). Then the modal characteristics of the fan rotor model are analysed using the (FEA) software ANSYS Workbench. Also, to study the effect of blade wear on critical speeds, Campbell's diagram is obtained. Finally, harmonic analy-

Noureddine Aimeur, Noureddine Menasri
Computational Investigation of vibration Characteristics Analysis for Industrial Rotor

DOI 10.2478/ama-2022-0044

sis is performed to determine the magnitude of the rotor vortex at critical speeds obtained with and without blade wear.

2. MODELING OF THE FAN (FN 280)

2.1. Draft fan description

The FN 280 type fans are designed to transport hot gases with limited non-abrasive dust content,and may be categorised under suction type fans that are not accompanied by a suction box.

The fan consists of an impeller with an assembly shaft, 16 blades with a front flange and a rear flange, the shaft and two bearings. The bearings are ball bearings for the thrust roller. The basic designation is 22,332 with a C3 sail for bearing 1 and 22,328 with a C3 sail for bearing 2. It is upturned over the shaft. One of them, designed as a steering bearing, is installed near the engine.The other bearing is designed to move with reference to the body of this bearing, and the shaft is constructed of steel; both of these bearings are mounted in cast FLS bearing housings and mounted on the stool. A cooling turbine is mounted on the shaft close to the casing since the fans have to work at temperatures above 125 °C. The components of the fan casing are the casing itself, the front flange, the rear flange and the suction roof. The casing of the fan, sealed by stuffing rope, is fitted with an inspection hatch. The front flange is bolted to the casing. The technical data of the fan are shown in Tab. 1:

Tab. 1. The technical data of fan

Type	FN280	
Numbers of blades	16	
Temperature	84 C°	
velocity	985 RPM	
Bearing 1	K11= 32000[k/mm]	C11= 3.3[N. s/mm]
	K22 =12000[k/mm]	C22 =1.5 [N. s/mm]
Bearing 1	K11 =38900[k/mm]	C11= 2.6[N. s/mm]
	K22 =16000[k/mm]	C22 =1.5 [N. s/mm]

2.2. Geometric model

The data for the FN 280 fan were taken from the industries and all the parts were designed with SolidWorks program except the blade; since there were no data available for the blade, it was necessary to rely on the reverse design using the coordinate measuring machine (CMM) to obtain point cloud data through the PC-DMIS program, as shown in Fig. 1.

Fig. 1. (a) Impeller Blade; (b) Cloud data from.(CMM)coordinate measuring machine

These data were then exported to Geomagic Design X to obtain a final CAD model, and the fan parts were assembled using the SolidWorks software, as shown in Fig. 2. The model was then converted to a file (x_t) and imported into the ANSYS Workbench program for modal analysis and harmonic response analysis.
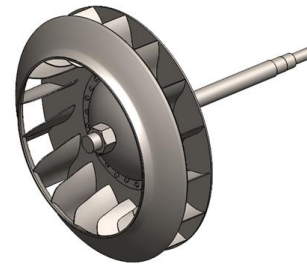

Fig. 2. CAD model of FN 280

2.3. Rotor dynamics equation

For modal analysis of multi DOF rotor bearing system, the equation of motion may be written as under:

$$[M]\{\ddot{u}\}+([D]+[G])\{\dot{u}\}+([S]+[H])\{u\}=\{F(t)\} \quad (1)$$

The positive definite, but not necessarily diagonal, matrix M is called the mass (inertia) matrix, the skew symmetric matrices G and H are referred to as the gyroscopic and circulatory matrices, respectively, and the indefinite non-symmetric matrices D and S are called the damping and the stiffness matrices, respectively. The matrices M, G, D and H are general rotational speed (Ω) dependent. For a given Ω, Eq. (1) can be written as:

$$[M]\{\ddot{u}\}+[C]\{\dot{u}\}+[K]\{u\}=\{f(t)\} \quad (2)$$

where the generalised damping and stiffness matrices, C and K, are now neither positive (negative) definite nor symmetric. We can assume, however, without loss of generality that M, C and K are real[22-23], and thus.

Either wouldbe a solution of the type:

$$W=Xe^{\lambda t}$$
$$A\lambda X+BX=0 \quad (3)$$

The gyroscopic effect is turned in software.

For harmonics response the equations of forced vibration are:

$$[M]\{\ddot{u}\}+[C]\{\dot{u}\}+[K]\{u\}=\{f(t)\} \quad (4)$$

$$f(t)=f_0\sin\omega t \quad (5)$$

3. BOUNDARY CONDITIONS

3.1. For modal analysis:

We apply a remote displacement condition for each bearing, constraining rotation and translation about the Z axis (bearings are in X–Y plane). We created bearings with the bearings' body-ground on the connection's context tab, their respective positions on the shaft and with stiffness and damping as indicated in Tab. 1.The Fig. 3. shows the position of the boundary condi-

tions applied to the rotor.

Considering that the maximum operating speed of the rotor is 985 rpm, a modal analysis was carried out at three different speeds in both cases; the first speed is 100 rpm, the second 600 rpm and the third 1,200 rpm.

3.2. For harmonic response analysis:

We apply the condition of remote displacement to the bearing locations, and the rotational and transition degrees of freedom are restricted about the Z axis at the bearing sites. Due to the possibility of resonance, and because the mass is asymmetric at the blades, it is converted into a point mass located in the position of the centre of mass, and the range of variance is determined. The frequency for harmonic response analysis is 0–70 Hz, and 2.333 Hz is set as one step for a total of 30 steps.
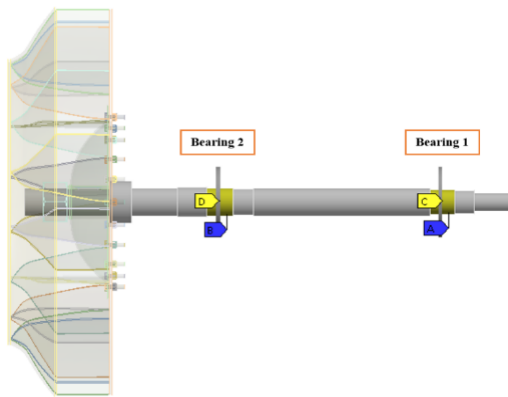
Fig. 3. Rotor boundary conditions

4. MESHING

One of the most important operations of ANSYS is the meshing process, which must be done correctly to enable an accurate simulation using (FEA). The mesh consists of elements containing nodes representing the shape of the geometry and can vary according to the element type. Based on the principle of performing calculations at a finite number of elements and then interpolating the results to the full size, any continuous object can have a large number of degrees of freedom, which makes it difficult to solve for (FEA), and by using division or entanglement, (FEA) reduces degrees of freedom from unlimited to limited. For meshing, there are several methods in the ANSYS workbench, including the mechanical method, the tetrahedral method and the hexahedral dominance method [24-25].
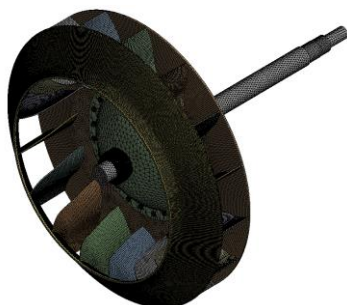

Fig. 4. Rotor mesh

The shaft components have been meshed with element SOLID185, which has the ability to be used in mixed forging, thus enabling the simulation of deformations of elastic materials that are almost incompressible. For blade modelling, the contact surfaces are first constructed at the parts' locations connected individually by the elements CONTA174 and TARGE170, and the bearings mesh with the COMBI214 element.

A total of 531,890 elements have been created and 239,491 nodes are shown in the meshing. Fig. 4 shows the figure of a meshed model.

5. RESULTS

5.1. Modal analysis

The model analysis was carried out at three different speeds: 100 rpm, 600 rpm and 1200 rpm. Additionally, a maximum of four modes was reckoned as ideal for carrying out the model analysis. Based on these parameters, the natural frequencies were calculated and a Campbell diagram was drawn to calculate the critical velocities of the rotor. The natural frequencies obtained from the typical analysis of the rotor are shown in Tab. 2. We note that values close to each other are obtained for the natural frequencies recorded in modes 1–3 at different speeds. As for mode 4, the natural frequency recorded at 1,200 rpm was greater than those at other speeds.

Tab.2. Natural frequencies rotor

Mode N°	Rotational Velocity [RPM]	Natural Frequency [Hz]
1		12.775
2	100	16.857
3		27.826
4		30.153
1		12.712
2	600	16.677
3		23.338
4		36.52
1		12.448
2	1200	15.911
3		19.959
4		45.71

5.1.1. Campbell diagram

The model analysis allows us to extract the Campbell diagram, as shown in Fig. 5, to analyse the evolution of frequencies at the speed of rotation and to determine the critical velocities and stability threshold.

We note that there are three critical speeds: 758.54 rpm, 972.12 rpm and 1,198.2 rpm, at frequencies of 12.775 Hz, 16.677 Hz and 19.959 Hz, respectively, and the following Tab. 3 represents the different rotational speeds obtained, together with values indicating the stability and rotation characterising each mode.
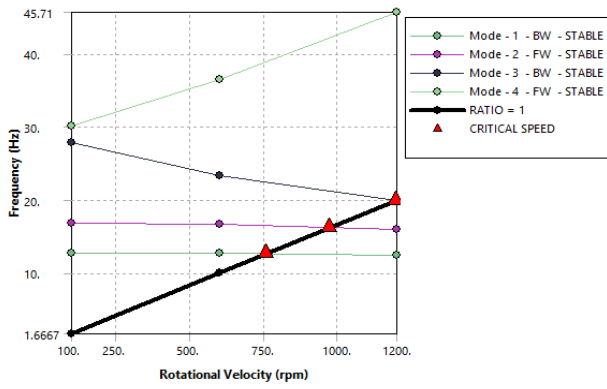
Noureddine Aimeur, Noureddine Menasri
Computational Investigation of vibration Characteristics Analysis for Industrial Rotor

DOI 10.2478/ama-2022-0044

Fig. 5. Campbell diagram

Tab.3. Critical speeds for different rotational speeds

Mode	Whirl Direction	Mode Stability	Critical Speed	100. rpm	600. rpm	1200. rpm
1	BW	STABLE	758.54 rpm	12.775 Hz	12.712 Hz	12.448 Hz
2	FW	STABLE	972.12 rpm	16.857 Hz	16.677 Hz	15.911 Hz
3	BW	STABLE	1198.2 rpm	27.826 Hz	23.338 Hz	19.959 Hz
4	FW	STABLE	NONE	30.153 Hz	36.52 Hz	45.71 Hz

5.1.2. Mode Shapes

Fig. 6. shows the modes of vibrations obtained at a rotational speed of 100 rpm.
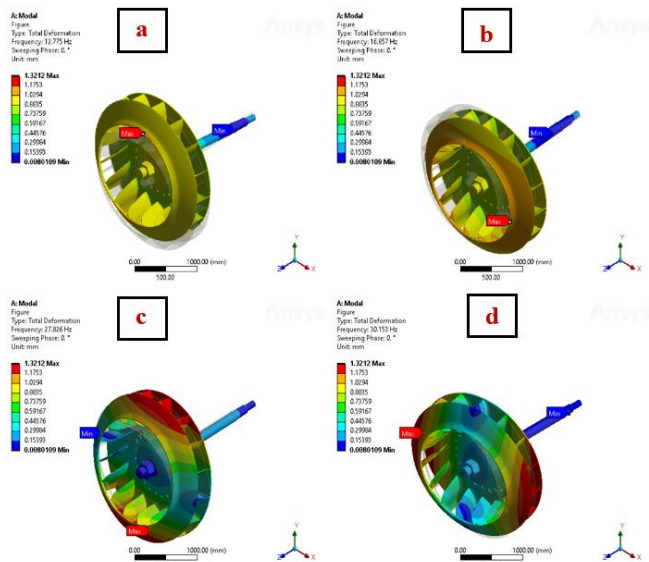
Fig. 6. The mode shapes of vibrations for speeds at 100 rpm:
(a) mode 1; (b) mode 2; (c) mode 3; (d) mode 4

Fig. 7. shows the modes of vibrations obtained at a rotational speed of 600 rpm.
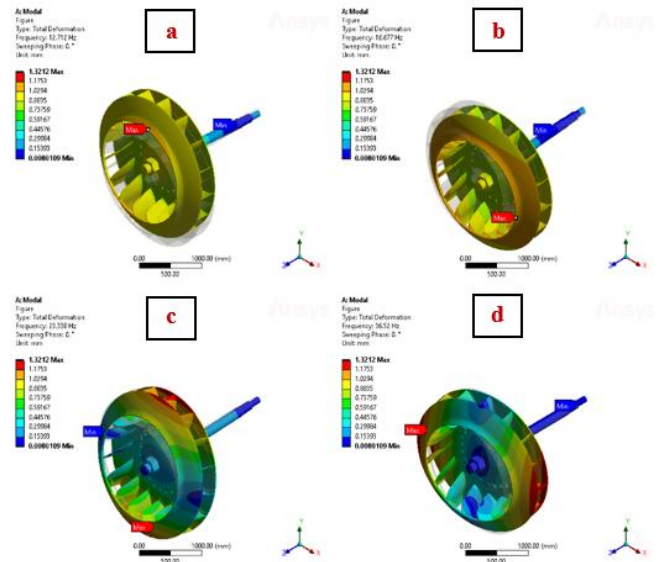
Fig. 7. The mode shapes of vibrations for speeds at 600 rpm:
(a) mode 1; (b) mode 2; (c) mode 3; (d) mode 4

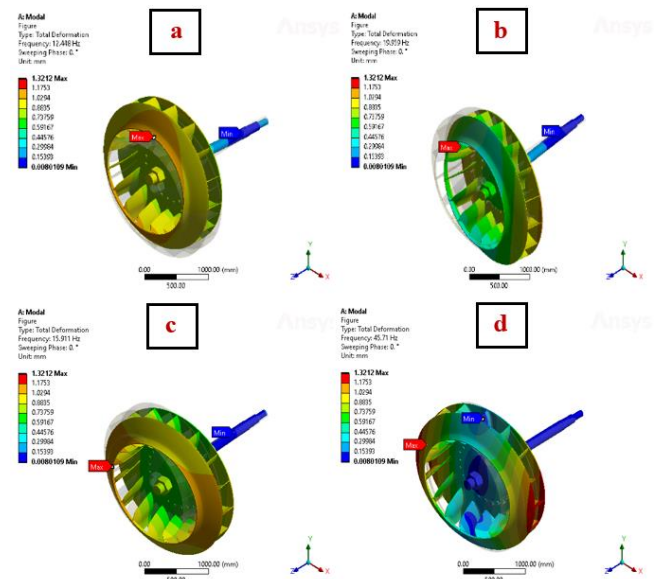Fig. 8. shows the modes of vibrations obtained at a rotational speed of 1,200 rpm.

Fig. 8. The mode shapes of vibrations for speeds at 1,200 rpm:
(a) mode 1; (b) mode 2; (c) mode 3; (d) mode 4

As for the form of vibration mode, it was found that the maximum distortion at different speeds is almost the same, where the maximum distortion at the first speed is 100 rpm, and the maximum distortion from the first to the fourth positions is in the range of 1.0418–1.5014 mm.

As for the second rotational speed of 600 rpm, the maximum distortion from the first to the fourth positions is in the range of 1.0506–1.338 mm.

As for the third rotational speed of 1200 rpm, the maximum deformation from the first to the fourth positions is in 1.0816–1.3212 mm.

5.2. Harmonic analysis

The harmonic response analysis of the rotor allows us to determine the deformation, stresses and effect of phase angle due to balanced and unbalanced forces acting on the shaft system. The harmonic analysis was carried out to show the frequency response arising pursuant to the application of an unbalanced force of 12,192 kg. mm at the centre of the disc in the two study cases.

5.2.1. Frequency response

Figs. 9–11 represent the severity of the deformation in the three directions.
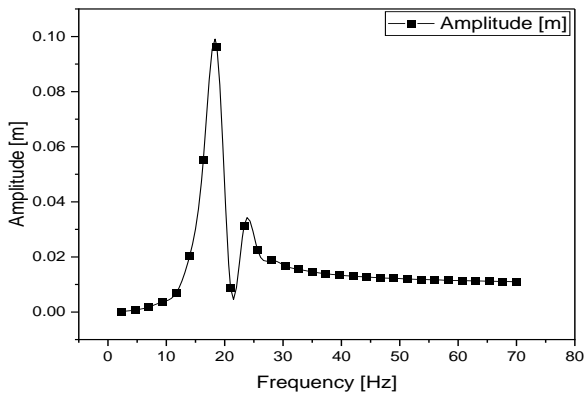
Fig. 9. Frequency response for X-direction
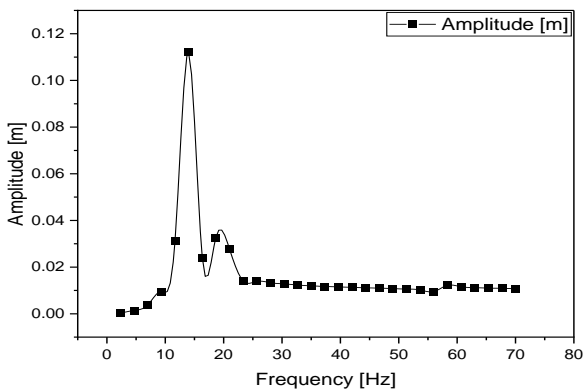
Fig. 10. Frequency response for Y-direction
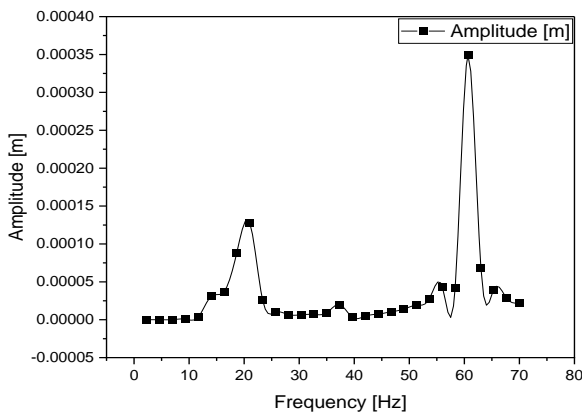
Fig. 11. Frequency response for Z-direction

In Fig. 9, we notice that the maximum amplitude of deformation in the X-direction is 9.6346e–005 m and it appears near 18.667 Hz, which is a value close to the natural frequencies of order 3.In the Y-direction, the maximum amplitude of deformation is 1.1213e–004 m, as shown in Fig. 10, and it appears that the frequency is approximately 14 Hz, which is close to the natural frequencies of the first order, while in the Z-direction, the maximum amplitude of deformation is 3.4939e–007 m, as shown in Fig. 11.

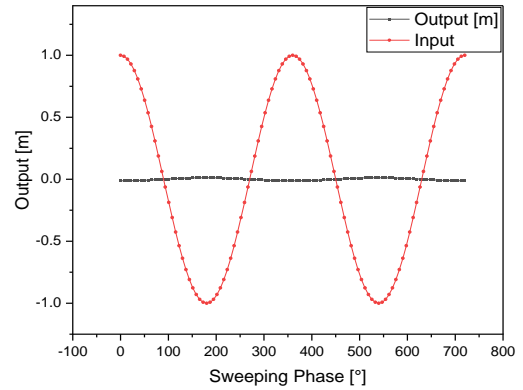### 5.2.2. Phase angle effect on deformation

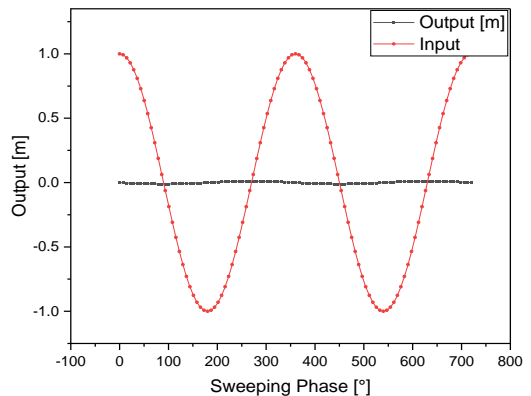**Fig. 12.** Phase Angle Directional Deformation X-direction

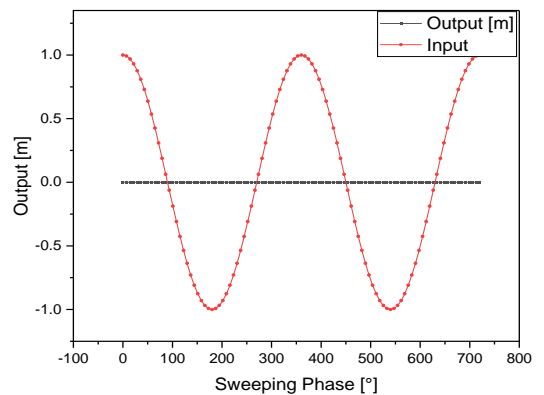**Fig. 13.** Phase Angle Directional Deformation Y-direction

Fig. 14. Phase Angle Directional Deformation Z-direction

The maximum phase angle is −179.78° at 45.71 Hz frequency in the X-direction, 90.25° at 45.71 Hz frequency in Y-direction and 129.02° at 45.71 Hz frequency in Z-direction.

Noureddine Aimeur, Noureddine Menasri
Computational Investigation of vibration Characteristics Analysis for Industrial Rotor

DOI 10.2478/ama-2022-0044

6. FAN WITH WORN BLADES

As the FN280 fan conveys hot gases with limited dust content (cement) over time, the fan blades erode over time. We wanted to simulate this tendency of the blades to undergo wear over time, as well as the worn condition of the blades, in our modelling process, and accordingly, in performing the modal analysis and harmonic response, we tried to design the blades in the form in which they would present after wear, the intent being to achieve a shape for the blades that would approximately correspond to their actual shape in reality post the expected duration of wear. Considering these requirements, the parts were assembled using SolidWorks software, as shown in Fig. 15.
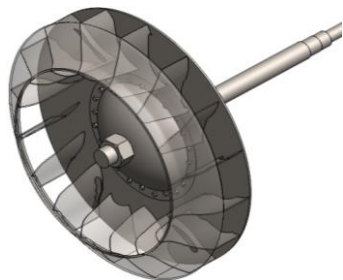

Fig. 15. CAD model of FN 280 with a worn blade

For the boundary conditions of the modal analysis, the same conditions are used as in the first case, with three different speeds: 100 rpm, 600 rpm and 1,200 rpm. The same conditions are applied for the harmonic response analysis, and the range of variance is determined. Thefrequency for harmonic response analysis is 0–70 Hz, and 2.333 Hz is set as one step for a total of 30 steps.

6.1. Meshing with a worn blade

Shaft components have been meshed with element SOL-ID185, which has the ability to be applied in mixed forging, thus enabling simulation of the deformations of elastic materials thatare almost incompressible. For blades' modelling, the contact surfaces are first constructed at the parts' locations connected individually by the elements CONTA174 and TARGE170, and the bearings mesh with the COMBI214 element.

A total of 531,210 elements have been created and 238,299 nodes are shown in the meshing, Fig 16 shows the figure of a meshed model.
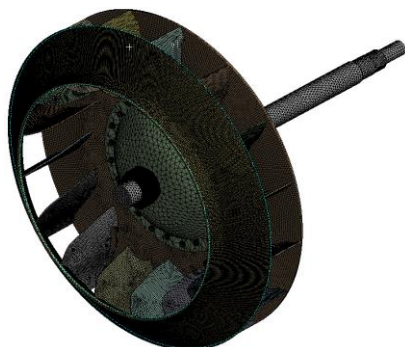

Fig. 16. Rotor mesh with a worn blade

6.2. Results

6.2.1. Modal Analysis

The model analysis was carried out at three different speeds: 100 rpm, 600 rpm and 1200 rpm, and a maximum of four nodes was used to perform the model analysis. Then, the natural frequencies were calculated and a Campbell diagram was drawn to calculate the critical velocities of the rotor. The natural frequencies obtained from the typical analysis of the rotor are shown in Tab. 4.We note that values close to each other are obtained for the natural frequencies recorded in modes 1–3 at different speeds. As for mode 4, the natural frequency recorded at 1200 rpm was greater than those at other speeds.

Tab. 4. Natural frequencies rotor with a worn blade

Mode N°	Rotational Velocity [RPM]	Natural Frequency [Hz]
1	100	13.501
2		18.155
3		30.945
4		33.399
5	600	13.478
6		18.071
7		26.252
8		39.62
9	1200	13.39
10		17.677
11		22.077
12		48.477

6.2.1.1. Campbell diagram

The model analysis allows us to extract the Campbell diagram, as shown in Fig. 17, to analyse the evolution of frequencies at the speed of rotation and to determine the critical velocities and stability threshold.
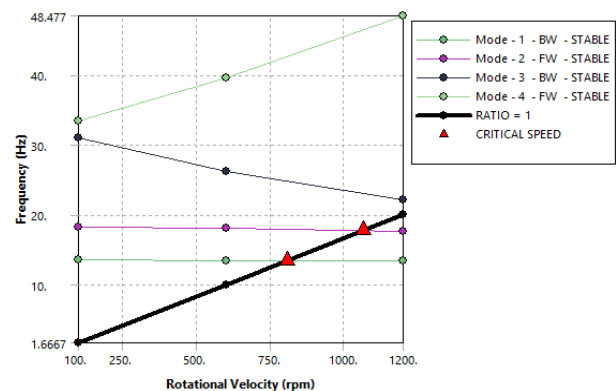

Fig. 17. Campbell diagram with a worn blade

We note that there are two critical speeds, 806.88 rpm and 1065.9 rpm, at frequencies 13.478 Hz and 18,071 Hz, respectively, and Tab. 5 represents the different rotational speeds obtained,

together with values indicating the stability and rotation character-ising each mode.

Tab.5. Critical speeds for different rotational speeds with a worn blade

Mode	Whirl Direction	Mode Stability	Critical Speed	100. rpm	600. rpm	1200. rpm
1	BW	STABLE	806.88 rpm	13.501 Hz	13.478 Hz	13.39 Hz
2	FW	STABLE	1065.9 rpm	18.155 Hz	18.071 Hz	17.677 Hz
3	BW	STABLE	NONE	30.945 Hz	26.252 Hz	22.077 Hz
4	FW	STABLE	NONE	33.399 Hz	39.62 Hz	48.477 Hz

6.2.1.2. Mode shapes

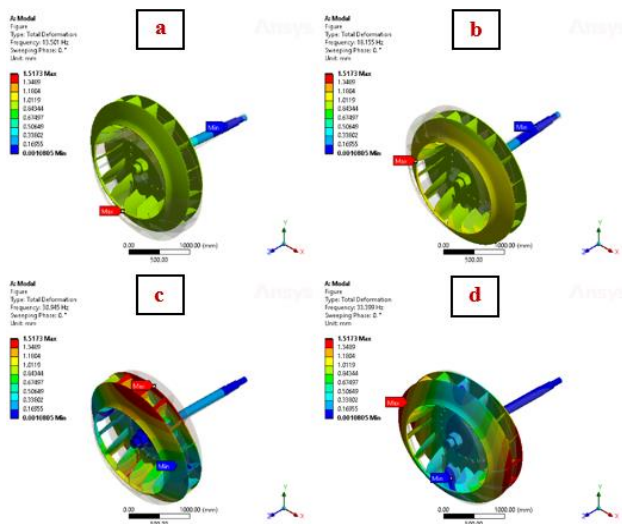Fig. 18. shows the modes of vibrations obtained at a rotational speed of 100 rpm.

Fig. 18. The mode shapes of vibrations for speeds at 100 rpm:
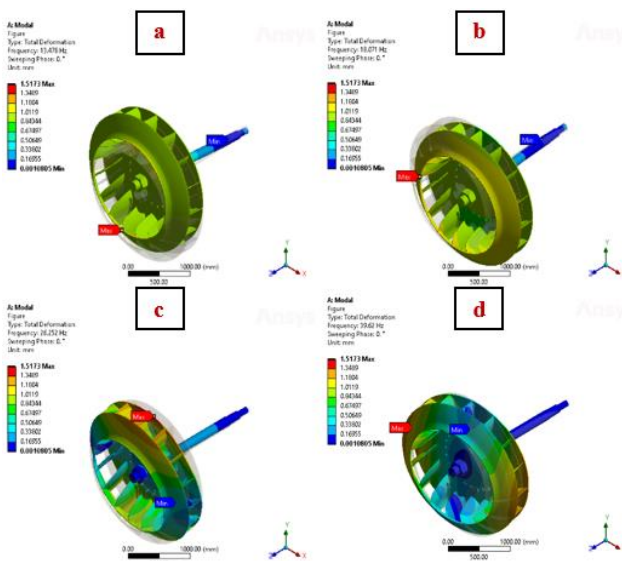(a) mode 1; (b) mode 2; (c) mode 3; (d) mode 4

Fig. 19. The mode shapes of vibrations for speeds at 600 rpm:
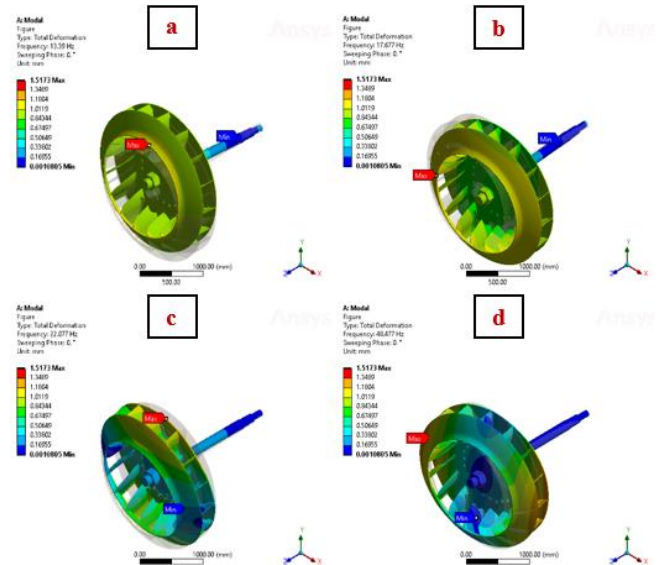(a) mode 1; (b) mode 2; (c) mode 3; (d) mode 4

Fig. 20. The mode shapes of vibrations for speeds at 1,200 rpm:
(a) mode 1; (b) mode 2; (c) mode 3; (d) mode 4

Fig. 19. shows the modes of vibrations obtained at a rotational speed of 600 rpm.

Fig. 20. shows the modes of vibrations obtained at a rotational speed of 1,200 rpm.

As for the form of vibration mode, it was found that the maximum distortion at different speeds is almost the same, where the maximum distortion at the first speed is 100 rpm, and the maximum distortion from the first to the fourth positionsin the range of 1.0184–1.7757 mm.

As for the second rotational speed of 600 rpm, the maximum distortion from the first to the fourth positions is in the range of 1.0228–1.5448 mm.

As for the third rotational speed of 1,200 rpm, the maximum deformation from the first to the fourth positions in the range of 1.0395–1.5173 mm.

6.2.2. Results of harmonic response analysis

6.2.2.1. Amplitude vs frequency

Figs. 21–23 represent the severity of the deformation in the three directions.
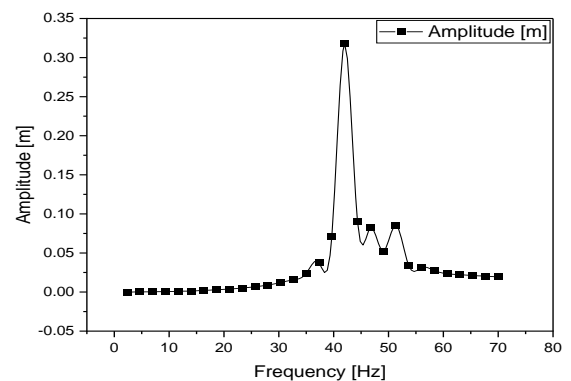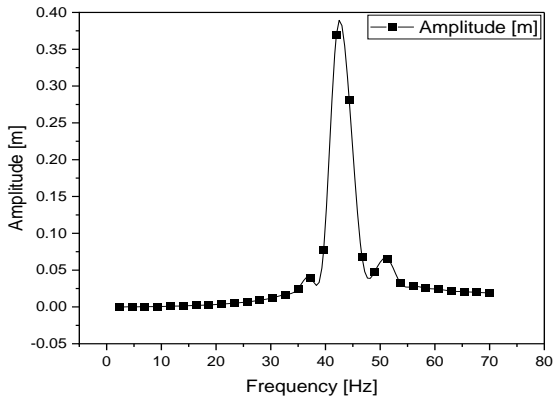

Fig. 21. Frequency response for X-direction

Noureddine Aimeur, Noureddine Menasri
Computational Investigation of vibration Characteristics Analysis for Industrial Rotor

DOI 10.2478/ama-2022-0044

Fig.2 2. Frequency response for Y-direction

Fig. 23. Frequency response for Z-direction

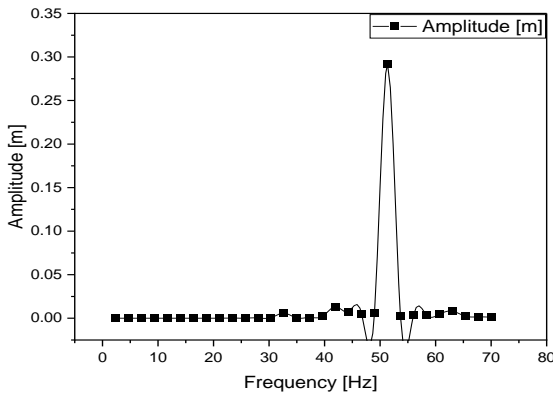**Fig. 25.** Phase Response Directional Deformation Y-direction
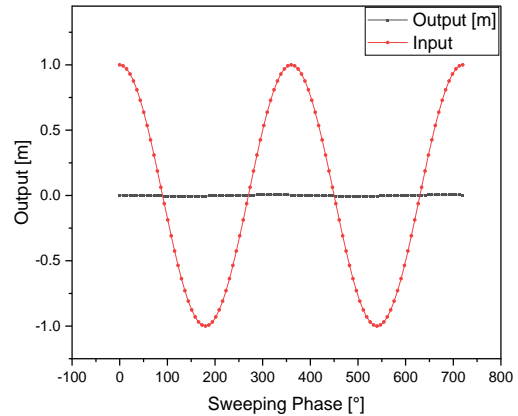

Fig. 26. Phase Response Directional Deformation Z-direction

In Fig. 21, we note that the maximum amplitude of deformation in the X-direction is 2.1737e–003 m, and it appears near the frequency of 16.33 Hz Fig. 21 and is close to the natural frequencies of the order 2. In Fig. 22, we note that the maximum amplitude of deformation in the Y-direction is 5.3828e–004 m, and it appears near the frequency 44.33 Hzand is close to the natural frequencies of order 4, while in Fig. 23, we note that the maximum amplitude of deformation in the Z-direction is 6.8784e–005 m, and it appears near the frequency 51.33 Hz and is close to natural frequencies of order 4.

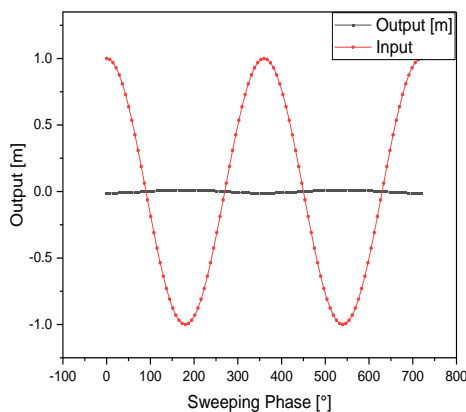#### 6.2.2.2. Phase angle effect on deformation

Fig. 24. Phase Response Directional Deformation X-direction

The maximum phase angle is 179.57° at 49 Hz frequency in X-direction, 89.82°at 49 Hz frequency in Y-direction and 40.241° at 49 Hz frequency in Z-direction.

7. CONCLUSIONS

In the present study, a rotating dynamic analysisof fan blades (FN 280 cement draft fan), in their normal state and in the state after corrosion, was performed using the finite element software ANSYS workbench, to ascertainnatural frequencies and critical speeds after obtaining Campbell's diagram in each case, and the following conclusions were drawn:

– The natural frequencies in the case of the natural fan are less than the value of the natural frequencies in the case after corrosion of the fan blades in all modes, and the maximum deformation in all vibration modes in the first case is less than in the case after corrosion of the fan blades.

– After the Campbell diagram was obtained in the case of the natural fan, three critical speeds were found at 758.54 rpm, 972.12 rpm and 1,198.2 rpm and these occurred in the operating range, but in the case of the fan after corrosion of the fan blades, two critical speeds were found at 806.88 rpm and 1,065.9 rpm.

– In the harmonic analysis, as a result of the unbalanced force of 12,192 kg.mm acting on the disk, the intensity of vibrationwas very high. In the case of a normal fan in the X-direction the system resonates when the excitation frequency reaches 18.667 Hz and 23.33 Hz and the vibration response reaches a

maximum at a frequency of 18.66 Hz; in the Y-direction it resonates at frequencies of 14 Hz and 18.667 Hz and reaches its maximum at 14 Hz; and in the Z-direction it resonates at frequencies of 21 Hz and 60.667 Hz, and reaches its maximum at 60.667 Hz. In the case of the fan after corrosion of the fan blades, the system resonates and reaches its maximum at a frequency of 16.33 Hz in the X- and Y-directions, in the Z-direction, resonates and reaches its maximum at an excitation frequency of 55.33 Hz.

REFERENCES

1. Kushwaha N, Patel V. Modelling and analysis of a cracked rotor: a review of the literature and its implications. Arch Appl Mech. 2020;90(6):1215-45.
2. Xie F, Aly A-M. Structural control and vibration issues in wind turbines: A review. Eng Struct. 2020;210:110087.
3. Gunter E. Critical speed analysis of offset jeffcott rotor using english and metric units. RODYN Vib Inc, Charlottesville, VA. 2004.
4. Cao H, Niu L, Xi S, Chen X. Mechanical model development of rolling bearing-rotor systems: A review. Mech Syst Signal Process. 2018;102:37-58.
5. Huaitao S, Jizong Z, Yu Z, Gang H, editors. Calculation and analysis of critical speed of high speed motor spindle rotor system. IOP Conf Ser Mater Sci Eng; 2018: IOP Publishing.
6. Lee C-W. Vibration analysis of rotors: Springer Science & Business Media; 1993.
7. Wang C, Zhang D, Ma Y, Liang Z, Hong J. Theoretical and experimental investigation on the sudden unbalance and rub-impact in rotor system caused by blade off. Mech Syst Signal Process. 2016;76:111-35.
8. Cardillo L, Corsini A, Delibra G, Rispoli F, Sheard AG, Venturini P. Predicting the performance of an industrial centrifugal fan incorporating cambered plate impeller blades. Period Polytech Mech Eng. 2014;58(1):15-25.
9. Krishna BRV, Mudgala S, Seth D. A comparative dynamic analysis of rotor involving three engineering materials applying finite element analysis (FEA) simulation. Mater Today Proc. 2021;47:4003-14.
10. Hnin MT, Htike TM. Investigation of natural frequency and critical speed for Jeffcott rotor system. J Res Appl Mech Eng. 2021;9(1).
11. Nan JY, Wang M, Zan T, Zhang JX, editors. Vibration Characteristics Analysis of a High-Speed Horizontal Machining Center. Adv Mater Res; 2012: Trans Tech Publ.
12. Khan MM, Shailesh P, Prasad M. Rotor Dynamic Analysis Of Driving Shaft Of Dry Screw Vacuum Pump. 2019.
13. Khamari DS, Kar PS, Jena S, Kumar J, Behera SK, editors. Rotordynamic Analysis of High-Speed Rotor Used in Cryogenic Turboexpander Using Transfer Matrix Method. Proceedings of the 6th National Symposium on Rotor Dynamics; 2021: Springer.
14. Bai B, Zhang L, Guo T, Liu C. Analysis of dynamic characteristics of the main shaft system in a hydro-turbine based on ANSYS. Procedia Eng. 2012;31:654-8.
15. Sinha JK, Lees A, Friswell M. Estimating unbalance and misalignment of a flexible rotating machine from a single run-down. J Sound Vib. 2004;272(3-5):967-89.
16. Yadav H, Upadhyay S, Harsha S. Study of effect of unbalanced forces for high speed rotor. Procedia Eng. 2013;64:593-602.
17. Fegade R, Patel V, Nehete R, Bhandarkar B. Unbalanced response of rotor using ansys parametric design for different bearings. Int J Eng Sci Emerg Technol. 2014;7(1):506-15
18. Khawaja H, Andleeb Z, Moatamedi M. Multiphysics based Modal and Harmonic Analysis of Axial Turbines. Int J Multiphysic. 2022;16(1):81-94.
19. Shuming L, Yujia W, editors. Damping Optimization of High Pressure Rotor Support Based on Harmonic Response Analysis. J Phys Conf Ser; 2021: IOP Publishing.
20. Nagaraj B, Patil L, Kamanat PK, Dhuri K, Azam MS. Rotordynamic Analysis of Bolted Disk-Drum Rotor with Contact Nonlinearity.
21. Xu H, Wang YQ. Differential transformation method for free vibration analysis of rotating Timoshenko beams with elastic boundary conditions. Int J Appl Mech. 2022;14(6):21.
22. Chong-Won L. Vibration analysis of rotors. SOLID Mech ITS Appl. 1993;21:156.
23. Ansys. Rotordynamic Analysis Guide. 2021:158.
24. Grunwald B. Vibration analysis of shaft in SolidWorks and ANSYS. 2018.
25. Mansoora HI, Al-Shammari M, Al-Hamood A, editors. Theoretical Analysis of the Vibrations in Gas Turbine Rotor. IOP Conf Ser Mater Sci Eng; 2020: IOP Publishing.

Noureddine Aimeur: https://orcid.org/0000-0003-0293-8417

Noureddine Menasri: https://orcid.org/0000-0002-7373-684X